

## MODELLING OF THE BINARY ALLOYS SOLIDIFICATION PROCESS WITH CONSTITUTIONAL UNDERCOOLING CONDITION

*Ewa Węgrzyn-Skrzypczak, Tomasz Skrzypczak*

*Institute of Mathematics and Computer Science, Czestochowa University of Technology, Poland  
email: skrzyp@imipkm.pcz.czest.pl*

**Abstract.** In the paper mathematical and numerical model of binary alloy solidification process is proposed. The metal alloy is viewed as mixture of basic component and solute. The approach basing on moving, sharp phase interface between liquid and solid region is introduced. Constitutional undercooling phenomenon is taken into consideration.

### Introduction

The most popular approaches of solidification process modelling include concept of two-phase zone which is located between liquidus and solidus isolines. These models are usually basing on enthalpy formulations [1-4] where motion of the liquid phase is neglected. The more complex and complicated models consider both the fluid flow and heat transfer phenomena [5]. Another group of solidification models reviewed in [6] are named as micro-macroscopic models. Interesting approach to modelling dendritic solidification basing on equilibrium solidification method is presented in [7].

Moving internal boundary is characteristic for Stefan problems. Mathematical model of solidification process with sharp interface between solid and liquid phase has its origin in the Lamé's and Clapeyron's works from 1831.

The solution of the binary alloy solidification problem with sharp interface is based on the solution of heat conductivity and mass diffusion equations with appropriate boundary, initial and continuity conditions. Mass and heat flux continuity conditions must be satisfied on the moving solidification front. Such process leads to instabilities appearing on the flat surface between solid and liquid region [8, 9]. These phenomena are responsible for mushy zone formation. Proposed numerical method basing on Finite Element Method [10-12] allows to predict loss of stability of moving planar front during solidification of any binary alloy.

## 1. Formulation of the problem

Sharp solidification interface separates solid and liquid subregions (Fig. 1).  $\Gamma_1$ ,  $\Gamma_2$  and  $\Gamma_3$  represent outer boundaries of the solidifying region and  $\Gamma_{l-s}$  determines location of the phase interface.

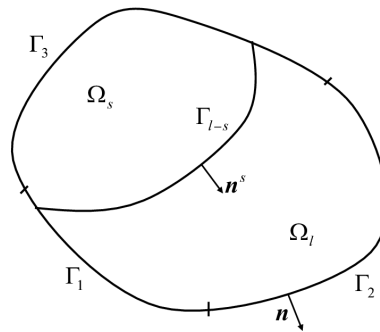


Fig. 1. Solid and liquid subregion in considered domain

Conventional description of the solidification process with sharp phase interface is based on the conservation equations written separately for liquid and solid phase. They are supplemented by boundary, initial and continuity conditions on the solidification front. Solutions of conventionally stated problem aren't effective and restricted to simplified cases of solidification [13, 14].

Many methods using for tracking the phase interface include mesh adapting. In proposed model one set of differential equations is solved for whole domain and calculations are performed on fixed grid. Jump in heat and mass fluxes on the internal boundaries are included using finite elements with interior discontinuities. Heat transport (1), mass diffusion (2) and level set equations (3) are coupled by heat and mass continuity equations (10)-(11) and govern the mathematical model of the process.

$$\nabla \cdot (\lambda_j \nabla T^j) = (c\rho)_j \frac{\partial T^j}{\partial t} \quad (1)$$

where  $T$  [K] denotes temperature,  $t$  [s] - time,  $\lambda$  [W/mK] - thermal conductivity,  $c$  [K/kgK] - specific heat,  $\rho$  [kg/m<sup>3</sup>] - density, whereas  $j$  represents liquid ( $l$ ) and solid ( $s$ ) phase.

$$\nabla \cdot (D_j \nabla C^j) = \frac{\partial C^j}{\partial t} \quad (2)$$

where  $C$  [-] represents solute concentration, while  $D$  [m<sup>2</sup>/s] is mass diffusion coefficient

$$V_n |\nabla \phi| + \frac{\partial \phi}{\partial t} = 0 \quad (3)$$

where  $\phi$  [m] is called distance function and  $V_n$  [m/s] denotes velocity normal to the solidification front calculated using following formula

$$V_n = \mathbf{n}^s \cdot \mathbf{v} = \frac{\nabla \phi}{|\nabla \phi|} \cdot \mathbf{v} \quad (4)$$

where  $\mathbf{v}$  represents velocity vector.

Equations (1)-(3) are completed by appropriate boundary conditions:

$$T^j \Big|_{\Gamma_1} = T_b, \phi \Big|_{\Gamma_{l-s}} = 0 \quad (5)$$

$$-\lambda_j \frac{\partial T^j}{\partial n} \Big|_{\Gamma_2} = q_T, D_j \frac{\partial C^j}{\partial n} \Big|_{\Gamma_{2-3}} = 0 \quad (6)$$

$$-\lambda_j \frac{\partial T^j}{\partial n} \Big|_{\Gamma_3} = \alpha(T - T_\infty) \quad (7)$$

where  $T_b$  [K] is known temperature on the boundary  $\Gamma_1$ ,  $q_T$  [W/m<sup>2</sup>] represents given heat flux over boundary  $\Gamma_2$ ,  $\mathbf{n}$  is a vector normal to the external boundary,  $\alpha$  [W/m<sup>2</sup>K] denotes heat transfer coefficient and  $T_\infty$  [K] is ambient temperature.

Initial conditions are defined as follows:

$$T \Big|_{t=0} = T_0, C \Big|_{t=0} = C_0, \phi \Big|_{t=0} = \phi_0 \quad (9)$$

where  $T_0$  [K],  $C_0$  [-],  $\phi_0$  [m] are initial temperature, solute concentration and distance function respectively.

Presented model is completed by continuity conditions on  $\Gamma_{l-s}$ :

$$T^s \Big|_{\Gamma_{l-s}} = T^l \Big|_{\Gamma_{l-s}} = T_L(C) \quad (10)$$

$$\lambda_s \frac{\partial T^s}{\partial n^s} \Big|_{\Gamma_{l-s}} - \lambda_l \frac{\partial T^l}{\partial n^s} \Big|_{\Gamma_{l-s}} = \rho_s L V_n \quad (11)$$

$$D_s \frac{\partial C^s}{\partial n^s} \Big|_{\Gamma_{l-s}} - D_l \frac{\partial C^l}{\partial n^s} \Big|_{\Gamma_{l-s}} = (C_L - C_S) V_n \quad (12)$$

where  $\mathbf{n}^s$  denotes vector normal to  $\Gamma_{l-s}$ ,  $L$  [J/kg] - latent heat of solidification,  $T_L(C)$  [K] - liquidus temperature and  $C_L, C_S$  [-] - solute concentration in the liquid and solid on  $\Gamma_{l-s}$ .

## 2. Examples of calculation

Geometry, boundary and initial conditions of the casting with selected nodes are presented in Figure 2. Cooling curves were prepared for these points on the basis of obtained results. Initial temperature of the liquid Fe-C alloy with 0.55% of carbon was 1800 K, material properties are compiled in Table 1.

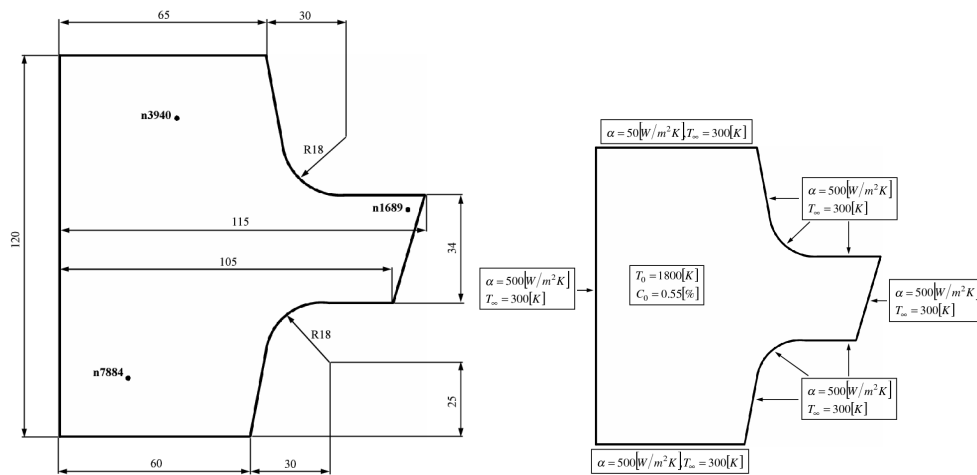


Fig. 2. Geometry of casting, boundary and initial conditions

Table 1

Material properties of Fe-C alloy

Material property	Solid phase	Liquid phase
$\lambda$	35	23
$\rho$	7800	6915
$c$	644	837
$D$	0	$2 \cdot 10^{-7}$
$L$	-	$2.7 \cdot 10^5$

Calculation process during early phase after mould pouring was performed with constant time step  $\Delta t = 0.001$  s. The value of  $\Delta t$  was calculated dynamically during solidification process.

Cooling process of the casting was modelled by Newton's boundary conditions (Fig. 2). On the top of the casting intensity of cooling was ten times lower than on the others. The influence of initial overheating on solidification process and super-cooled zone was investigated.

In Figure 3a-b temperature field after 31.4 and 128.8 s are presented. Position of solidification front is marked with dashed line. The most intensive cooling process can be observed along external boundaries, especially near the bottom corners and in the narrow region on the right side of the casting. Solid phase appears in the most right corner after one second of simulation start.

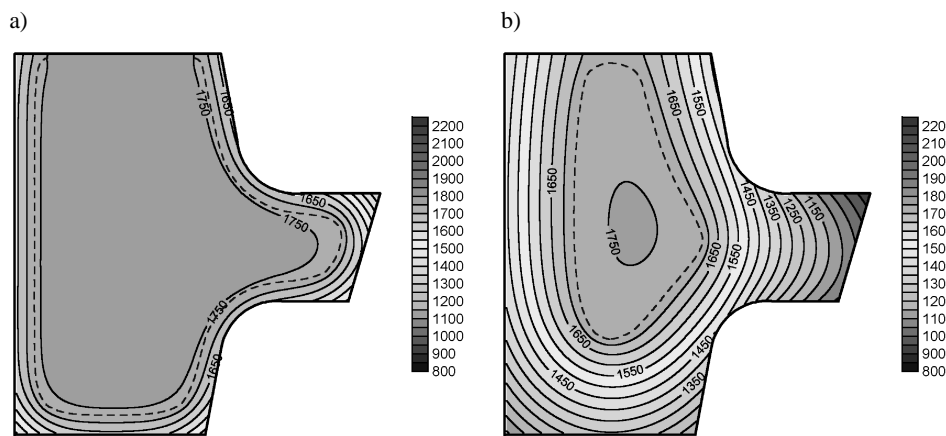


Fig. 3. Temperature field after: a) 31.4 s, b), 128.8 s

Solute concentration field after solidification process is presented in Figure 4a. The zone with higher concentration of solute is located in the central part of the casting. It starts on the top and leads down to the bottom of the casting. Concentration of carbon is also noticeable in the tapered part on the right side of the region. Position and shape of carbon-rich zones allow to predict impurities concentration and formation of casting defects (i.e. shrinkage cavities).

Cooling curves for selected nodes are presented in Figure 4b. Cooling rates near the liquidus temperature decrease due to phase change and latent heat emission. The moment when solidification front passes over particular node looks like a "step" on the cooling curve. This stage is much more evident for slow movement of phase interface than near the cooled boundaries where solidification front moves faster.

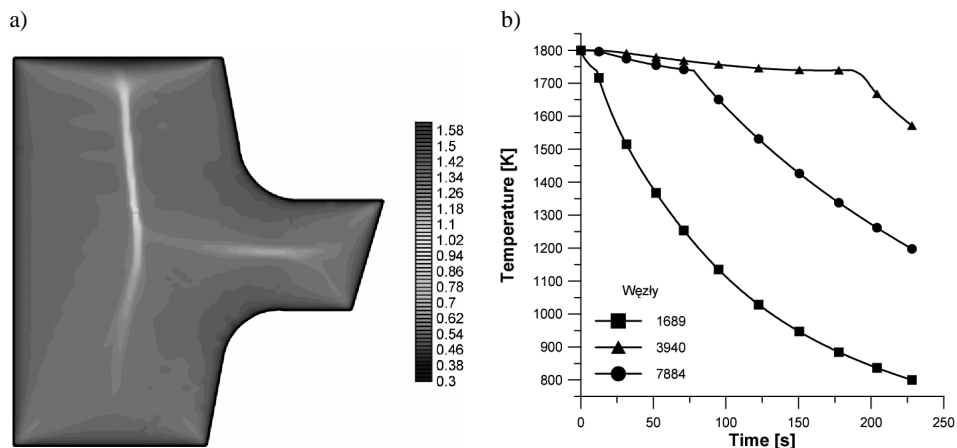


Fig. 4. Solute concentration after end of solidification (a), cooling curves prepared for selected nodes (b)

## Conclusions

Numerical modelling of binary alloys solidification process with constitutional undercooling criterion allows to predict loss of stability of the planar solidification front and undercooled zone evolution. Computer program was implemented on the base of optimized solute segregation algorithm and fast front tracking method. Obtained results contain temporary front position, temperature and solute distribution and allow to analyse solidification process depended on particular material and technological parameters.

## References

- [1] Szczygiol N., Szwarc G., Application of enthalpy formulations for numerical simulation of castings solidification, *Computer Assisted Mechanics and Engineering Sciences* 2001, 8, 99-120.
- [2] Szczygiol N., Approaches to enthalpy approximation in numerical simulation of two-component alloy solidification, *Computer Assisted Mechanics and Engineering Sciences* 2000, 7, 717-734.
- [3] Mochnacki B., Suchy J.S., Numerical methods in computations of foundry processes, Polish Foundrymen's Technical Association, Kraków 1995.
- [4] Szczygiol N., Modelowanie numeryczne zjawisk termomechanicznych w krzepącym odlewie i formie odlewniczej, Wydawnictwo Politechniki Częstochowskiej, Częstochowa 2000.
- [5] Parkitny R., Sowa L., Numerical simulation of solidification of a casting taking into account fluid flow and heat transfer phenomena. The axisymmetrical problem, *Journal of Theoretical and Applied Mechanics* 2001, 39(4), 909-921.
- [6] Rappaz M., Modeling of microstructure formation in solidification processes, *Int. Mater. Rev.* 1989, 34(3), 93-123.
- [7] Wesołowski Z., Parkitny R., One dimensional model of slow solidifying of cast metal, *Biulletin of the Polish Academy of Sciences* 1997, 45(4), 513-524.

- [8] Parkitny R., Bokota A., Supernat K., Analiza stabilności płaskiego frontu krzepnięcia dla liniowego i pierwiastkowego prawa narastania, *Solidification of Metals and Alloys* 2002, 2, 204-209.
- [9] Parkitny R., Supernat K., Analysis of concentration super-cooling in general Stefan question, *Solidification of Metals and Alloys* 1998, 38, 43-48.
- [10] Zienkiewicz O.C., *The Finite Element Method*, McGraw Hill, London 1977.
- [11] Majchrzak E., Mochnacki B., *Metody numeryczne: Podstawy teoretyczne, aspekty praktyczne i algorytmy*, Wydawnictwo Politechniki Śląskiej, Gliwice 1994.
- [12] Bathe K.J., *Finite element procedures in engineering analysis*, Prentice-Hall, Englewood Cliffs 1982.
- [13] Rubinstein L.I., *The mathematics of diffusion*, Oxford University Press, London 1959.
- [14] Tao L.N., On solidification of a binary alloy, *Quart. J. Mech. and Appl. Math.* 1980, 33.